Numerical Analysis of Weld Pool Fluid Flow in Laser+GMAW Hybrid Heat Source Welding Postprint

Authors: Xu Guoxiang, Zhang Weiwei, Liu Peng, Du Baoshuai

Date: 2016-11-05T00:00:00+00:00

Abstract

Considering the effects of droplets and keyhole on the molten pool, a three-dimensional transient numerical analysis model for molten pool fluid flow in laser+GMAW hybrid heat source welding was established based on FLUENT software. The arc heat input was described using a double ellipsoid heat source, while the laser heat input was treated as a hyperboloid of revolution heat source with adjustable heat flux peak, whose heat source distribution parameters were determined through a simplified keyhole shape and size model; the droplet transfer process was regarded as a process of high-temperature liquid metal flowing into the molten pool from a specific region at the upper part of the pool, and the droplet transfer frequency was characterized by establishing a periodic function of liquid metal flow velocity with respect to time; the keyhole was considered as surface deformation of the molten pool caused by laser-induced vapor recoil force to simplify the calculation process, focusing on the primary influence of keyhole existence on the molten pool fluid flow pattern.

Using the established model, simulations were conducted for keyhole morphology, molten pool fluid flow, and temperature field in laser+GMAW hybrid heat source welding under different welding conditions, the flow field characteristics of laser+GMAW hybrid welding were analyzed, and the influence patterns of laser power on the dynamic behavior of the hybrid welding molten pool were investigated.

The results show that under a welding speed of 1 m/min, hump defects appeared in GMAW welding (laser power of 0 W); when the laser power was 500 W, the hump defects disappeared, but no keyhole was generated in the molten pool, and the fluid flow pattern was similar to that of GMAW welding; whereas when the laser power increased to 2000 W, a keyhole appeared in the molten pool, making the fluid flow pattern more complex.

By comparing the calculated weld cross-section shape and dimensions with experimental results, good agreement was obtained, thereby demonstrating the accuracy and applicability of the model.

Full Text

Vol. 51, No. 6, June 2015, pp. 713-723

NUMERICAL ANALYSIS OF FLUID FLOW IN LASER+GMAW HYBRID WELDING

XU Guoxiang[1]), ZHANG Weiwei[1]), LIU Peng[1]), DU Baoshuai[2]) [1]) Key Laboratory of Advanced Welding Technology of Jiangsu Province, Jiangsu University of Science and Technology, Zhenjiang 212003 [2]) Shandong Electric Power Institute, Jinan 250062

Correspondent: XU Guoxiang, associate professor, Tel: (0511)84497208, E-mail: xugxiang@163.com Supported by National Natural Science Foundation of China (No. 51105182) and Open Fund for Jiangsu Provincial Key Laboratory for Advanced Welding Technology (No. 10622010101) Manuscript received 2014-08-19, in revised form 2014-12-31

ABSTRACT: Laser + gas metal arc welding (GMAW) hybrid welding fully combines the merits of both laser welding and GMAW, which can achieve high quality, high efficiency and comparatively low-cost welding of thin and thick plate, thus having great application prospect in manufacturing industry. However, compared with single heat source welding, hybrid welding involves more welding parameters and more complicated physical process, leading to difficult process optimization. When mismatching the process parameters, welding defects can still appear in high-speed welding, which affects the reliability of hybrid welding. Therefore, it is necessary to study the physical mechanism in hybrid welding deeply for suppressing welding defects and improving welding stability. In hybrid welding, fluid flow in weld pool has a critical influence on the weld formation. So, modeling and simulating the fluid flow is helpful for understanding the process mechanism completely. To date, however, there is only little study on velocity field in hybrid welding due to its complexity. In this work, with considering the effects of droplet and keyhole on weld pool, a three dimensional transient model is developed to numerically analyze fluid flow in weld pool of laser+GMAW hybrid welding based on FLUENT software. Arc heat input is modeled using an double-ellipsoid heat source; laser heat input is regarded as a hyperbolic curve-rotated heat source with changing peak power density, its distribution parameters being determined based on the simplified model for keyhole geometry and size. Droplet transfer is described as the process of high temperature liquid metal flowing into weld pool from the certain domain above the weld pool. Using the built model, the keyhole behavior, fluid flow and temperature distribution in laser+GMAW hybrid welding under different welding conditions are calculated. The features of velocity field in hybrid welding are analyzed and

the effect of laser power on the weld pool dynamic behavior is discussed. The results show that, in the case of 1 m/min, weld bead hump is generated in single GMAW (laser power 0 W); when laser power is 500 W, bead hump disappears in welding, but there is no keyhole emerging in hybrid weld pool and fluid flow pattern is close to that in GMAW. When increasing laser power to 2000 W, keyhole is formed, which makes the fluid flow in weld pool more complicated. The predicted weld geometries and dimensions for varied laser powers are compared with the measured data, which are in good agreement, thereby indicating accuracy and applicability of the established model.

KEY WORDS: hybrid welding, weld pool, fluid flow, keyhole, numerical simulation

Introduction

Laser + gas metal arc welding (GMAW) hybrid welding integrates the dual advantages of laser welding and GMAW, enabling high-speed, high-quality, and relatively low-cost welding of both thin and thick plates, which holds tremendous application prospects in industrial manufacturing [1~4]. However, compared with single heat source welding processes, hybrid welding involves numerous process parameters that are difficult to optimize [3~5]. Improper matching of process parameters can still lead to welding defects during high-speed welding, resulting in relatively poor process reliability and hindering its further promotion and application [5,6]. The fluid flow pattern in the weld pool is closely related to defects such as humping, undercut, and porosity, and exerts a critical influence on weld formation [6~8]. Therefore, conducting numerical analysis of fluid flow in the laser+GMAW hybrid welding weld pool is helpful for comprehensively understanding the formation mechanism of hybrid welding defects and optimizing process parameters, thereby improving welding process reliability. This research holds significant academic value and engineering practical importance.

During hybrid welding, coupling interactions exist among the laser-induced keyhole, droplets, and weld pool, making the fluid flow pattern in the weld pool more complex than in single heat source welding [9]. Consequently, current numerical simulation studies on laser+GMAW hybrid welding mechanisms have primarily focused on thermal fields [9~17] and stress fields [18~20], with very limited research on weld pool fluid flow. Moreover, existing studies have mainly concentrated on specific physical phenomena under particular welding conditions. Cho and Farson [8] simulated fluid flow and weld formation in laser+GMAW hybrid welding using a double-ellipsoid heat source and FLOW-3D software, but their study was only applicable to hybrid welding processes without keyhole formation. Cho et al. [21,22] established a three-dimensional numerical analysis model for laser+GMAW hybrid welding by combining a Gaussian planar heat source with a keyhole heat source, analyzing the fluid flow pattern under a single condition. However, their model did not consider the interaction between laser and arc, and the calculation results lacked experimental verification. Zhou

and Tsai [23] numerically analyzed the diffusion process of droplets after entering the keyhole in stationary hybrid welding using a two-dimensional numerical model, while Wang Renping [24] also simulated droplet transfer, arc, and weld pool in stationary hybrid welding using a two-dimensional model. Neither study addressed weld formation, and their models were not suitable for moving heat source welding or three-dimensional fluid flow analysis, thus limiting further application. Gao Zhiguo [25] numerically calculated fluid flow in aluminum alloy hybrid welding, but the calculation time was short (less than 0.2 s), and the results could not comprehensively reflect the characteristics of hybrid welding fluid flow and its influence on weld formation.

In this work, based on FLUENT software, an applicable three-dimensional transient numerical analysis model for weld pool fluid flow in laser+GMAW hybrid welding was established. The fluid flow pattern in hybrid welding was simulated and calculated, its characteristics were analyzed, and the influence of laser power on hybrid welding fluid flow and weld formation was investigated, thereby providing technical support and theoretical foundation for deeply understanding the internal mechanism of laser+GMAW hybrid welding and its engineering application.

Experimental Setup

The base material was 304 stainless steel plate with a thickness of 6 mm; the filler wire was 304 stainless steel wire with a diameter of 1.2 mm. [FIGURE:1] shows a schematic diagram of the laser+GMAW hybrid welding process. During hybrid welding, the laser was positioned ahead and perpendicular to the workpiece surface; the arc was behind at a 27° angle to the laser, with a laser-wire distance of 3 mm. The welding current was 170 A, arc voltage was 20 V, welding speeds were set at 1 and 2 m/min, laser powers were set at three levels of 0 (i.e., single GMAW), 500, and 2000 W, defocus amount was -1 mm, laser focal spot diameter was 0.2 mm, and the shielding gas was Ar+10%CO_2 (volume fraction).

2.1 Heat Source Models

2.1.1 Arc Heat Input - Double Ellipsoid Heat Source Model During welding, the weld pool surface (around the keyhole region) undergoes certain deformation under arc pressure and laser-induced vapor recoil force. Due to the relatively high welding speed in hybrid welding, a double ellipsoid heat source model was adopted to describe the arc heat input distribution pattern. In calculations, the heat source center was located on the workpiece surface, and its heat flux density distribution function qf(x, y, z) is expressed as follows: r = 2 where x, y, z are coordinates; af, ar, bh, ch are heat source distribution parameters; ff and fr are the heat distribution coefficients for the front and rear parts of the heat source, respectively; hA is arc heat efficiency; I is welding current; U is arc voltage; v is welding speed; and t is time.

2.1.2 Laser Heat Input - Conical Heat Source Based on Simplified Keyhole Model To improve computational efficiency and focus on numerical analysis of hybrid welding fluid flow, a hyperbolic curve-rotated heat source model with adjustable heat flux peak [14] was adopted to describe the laser heat flux distribution pattern. Its heat flux density distribution function qL(r, z) is expressed as follows: where r, z are coordinates, r y^2, hL is laser heat efficiency, PL is laser power, $r_0(z)$ is the heat source action radius, re and ri are the upper and lower surface radii of the heat source, ze and zi are the z-coordinates of the upper and lower surfaces, c is the proportionality coefficient for heat flux peak between upper and lower surfaces, a and b are calculation parameters, and A and B are process calculation parameters. Their specific calculation formulas are given in reference [14].

This model comprehensively considers the variation of laser heat input action region and heat flux peak along the workpiece thickness direction. Its action radius decreases hyperbolically along the thickness direction, while the heat flux density peak at the heat source central axis also varies hyperbolically along the thickness. When the proportionality coefficient c is greater than 1, the heat flux peak increases hyperbolically along the thickness direction; otherwise, it decreases. During calculation, the keyhole geometry and size are determined using a numerical analysis model for keyhole shape based on line heat source, and then the upper and lower surface radii and height of the heat source model are determined based on the keyhole size. The specific calculation steps are given in reference [15]. The influence of multiple reflections of laser inside the keyhole and Fresnel absorption of laser energy by the keyhole wall on laser energy distribution is indirectly considered by appropriately adjusting the proportionality coefficient c for heat flux peak between upper and lower surfaces of the volume heat source.

2.2 Droplet Transfer Model

To reduce computational cost while considering the influence of droplets on hybrid welding fluid flow, keyhole dynamic behavior, and heat distribution, a simplified droplet transfer model based on FLUENT software was established. In calculations, the droplet transfer process was treated as liquid metal flowing into the weld pool from the wire existence region above the weld pool at a certain velocity. This region area equals the wire cross-section area, i.e., assuming the droplet diameter equals the wire diameter. As shown in [FIGURE:2], the upper boundary of the workpiece solution domain was set as a velocity inlet for liquid filler metal. The initial inflow velocity of liquid metal (along the negative z-axis direction) was set in the wire action region (with area equal to the wire cross-section), while the velocity was zero elsewhere, indicating no liquid metal inflow in other regions, thereby characterizing the droplet transfer after wire melting. Similar to the heat source model, the wire action region moves along the welding direction according to the welding speed during calculation.

The liquid metal is only subject to gravity during inflow into the weld pool.

The influence of electromagnetic force and plasma flow force on droplet transfer velocity is indirectly considered by appropriately increasing the initial inflow velocity of liquid metal. Additionally, the droplet transfer frequency is simulated by applying a time-periodic function to the liquid metal inflow velocity. It is assumed that within one droplet transfer cycle, the liquid metal flow velocity is zero for half of the time. During calculation, the initial liquid metal velocity was set at 1 m/min, higher than that in reference [21]; the droplet transfer frequency was determined based on the wire feed speed, and the liquid metal temperature was assumed to be 2400 K [21].

2.3 Governing Equations and Boundary Conditions

The fluid flow in laser+GMAW hybrid welding is extremely complex, requiring simplifications for calculation. The following assumptions are proposed: (1) Except for thermal conductivity, specific heat, and dynamic viscosity coefficient, other material physical properties are temperature-independent; (2) The fluid in the weld pool is incompressible Newtonian fluid with laminar flow; (3) The pressure inside the keyhole is atmospheric pressure. The fluid in the weld pool flows under the action of arc pressure, surface tension, electromagnetic force, gravity, buoyancy, Marangoni force, laser-induced vapor recoil force, etc. The governing equations describing heat transfer and fluid flow in droplet-weld pool-keyhole include energy, momentum, and mass conservation equations, with specific expressions given in reference [26]. The enthalpy-porosity method [27] is used to simulate solidification and melting problems.

During hybrid welding, the keyhole has a strong stirring effect on the fluid in the weld pool, and the influence of keyhole dynamic behavior on hybrid welding fluid flow pattern must be considered in numerical simulation. The keyhole is treated as a deformation of the weld pool surface caused by the combined action of laser-induced vapor recoil force, arc pressure, and surface tension, ignoring the thermal and force fields of plasma inside the keyhole. During calculation, the following stress boundary condition exists on the free surface of the weld pool:

where P is the pressure acting on the weld pool free surface, PA is arc pressure, PR is vapor recoil force, and PS is surface tension. The arc pressure adopts a double elliptical distribution pattern [16]:

where m_0 is magnetic permeability; C is a calculation coefficient; aj_1, aj_2, bj, bj_1, bj_2 are arc pressure distribution parameters.

The laser-induced vapor recoil force is the main driving force for keyhole formation and can be expressed as [23]:

where A_0 and U_0 are calculation coefficients, B_0 is evaporation constant, Tw is weld pool surface temperature, ma is atomic mass, Lb is latent heat of evaporation, Na is Avogadro constant, and kb is Boltzmann constant.

Surface tension is expressed as:

where g is surface tension coefficient, k is free surface curvature radius, and its calculation formula is given in reference [26]. Since arc pressure, vapor recoil force, and surface tension are surface forces, they need to be converted to volume forces and applied as source terms in the momentum equation at the gas-liquid interface of the weld pool [21,24]. The required initial conditions and other energy and momentum boundary conditions are given in reference [21]; other forces such as electromagnetic force and buoyancy are treated according to the method in reference [7].

2.4 Weld Pool Free Surface

The VOF method is used to track the weld pool free surface. The control equation for the fluid volume function F is expressed as follows:

where u, v, w are fluid velocities in the x, y, z directions, respectively.

2.5 Solution Method

The fluid flow in hybrid welding was simulated using the computational fluid dynamics software FLUENT. Due to symmetry, half of the workpiece was taken as the calculation domain with dimensions of 50 mm × 20 mm × 9 mm, with 3 mm of air above (see [FIGURE:2]). The geometric model of the calculation domain was established using GAMBIT software and meshed. For the air region, except for the symmetry plane, the upper boundary was set as velocity inlet and other boundaries as pressure outlet; for the metal region, except for the symmetry plane, the other three boundaries were set as walls. User-defined functions were used to define boundary conditions (including initial velocity of high-temperature liquid metal flowing into the weld pool), material properties, and source terms for energy and momentum. In calculation, considering both accuracy and efficiency, variable time steps were adopted in this work, ranging from 10^{-4} to 10^{-6} s; the PISO algorithm (Pressure-Implicit with Splitting of Operators) was used to calculate the flow field.

3 Numerical Calculation of Fluid Flow in Hybrid Welding

Using the above model, fluid flow in laser+GMAW hybrid welding under different welding conditions was simulated via FLUENT software. The material physical properties and calculation parameters used in the calculations are given in references [23,26]. Model distribution parameters were determined according to the above method. For single GMAW welding (laser power 0 W, with the torch still at a certain angle to the workpiece), the model distribution parameters were: af = 4 mm, ar = 6 mm, bh = 4 mm, ch = 2 mm, aj_1 = 3 mm, aj_2 = 4 mm, bj = 3 mm. Model distribution parameters for other process conditions were also determined according to the above method.

[FIGURE:3] shows the calculated fluid flow in the longitudinal section of the weld pool for single GMAW welding. It can be seen that due to the high

welding speed, under arc pressure, the fluid at the front of the weld pool rapidly flows toward the rear, reaching a maximum velocity of 2.5 m/s, while a large depression forms in the arc-affected region at the front of the weld pool. The liquid metal layer at the front wall of the depression is very thin, and the liquid metal at this location flows toward the bottom of the depression at high speed. At t = 0.3 s, due to the small volume and short length of the liquid weld pool, the liquid metal at the bottom of the depression is expelled by arc pressure and flows backward from the bottom of the weld pool, generating a clockwise vortex near the heat source in the middle of the weld pool; while at the rear of the weld pool, a counterclockwise vortex is generated under the influence of surface tension and hydrostatic pressure, as shown in [FIGURE:3a]. As the arc heat source moves, liquid metal gradually accumulates at the rear of the weld pool, forming a thin metal transition region between the accumulation area and the front depression of the weld pool. The liquid metal in this region flows at high speed toward the rear of the weld pool and overcomes hydrostatic pressure, forming a counterclockwise vortex at the rear, as shown in [FIGURE:3b]. Since the liquid metal in the transition region has less heat and solidifies rapidly, and the thermocapillary stability in this region is poor, prone to transverse contraction [8], it hinders the flow of liquid metal from the front to the rear of the weld pool and the backflow of liquid metal from the accumulation region to the front, causing new metal accumulation at the front of the weld pool, as shown in [FIGURE:3c]. [FIGURE:3d] shows that at t = 2 s, due to the lower temperature in the transition region, less liquid metal flows from the front to the rear of the weld pool; under hydrostatic pressure, the liquid metal at the rear of the weld pool flows toward both the rear and front, while a counterclockwise vortex reappears at the front. When the liquid metal in the transition region solidifies, a humping defect forms in the weld. Since fluid flow in the weld pool is affected by multiple factors during welding, the flow pattern is prone to fluctuations, and only a specific moment flow pattern is presented here. [FIGURE:4] shows the calculated and experimental results of the weld bead top surface under this condition. It can be seen that the calculation results can better reflect the weld formation, thereby proving the accuracy of the model. It should be noted that the fluid flow pattern shown in [FIGURE:3] is the key factor for humping defect formation under the studied conditions, while the relationship between the peak flow velocity and humping defect formation is not obvious due to the influence of multiple factors such as welding speed and current. Additionally, humping defect formation is also affected by factors such as surface tension stability of liquid metal along the weld direction and material properties [8].

[FIGURE:5] shows the calculated temperature and flow fields in the cross-section of the GMAW weld pool at x = 21 mm. It can be observed that at t = 0.5 s, the workpiece metal is melted by arc heat and produces weld pool surface deformation under arc pressure, with liquid metal flowing toward the bottom of the weld pool. At t = 0.6 s, the surface depression of the weld pool is filled with liquid metal, and the liquid metal at the symmetry axis (y = 0) flows downward from the pool surface, which is related to the effect of electromagnetic force;

while the fluid at the pool surface slightly away from the symmetry axis flows toward the pool boundary under surface tension. As the heat source continues to move, the influence of arc pressure and electromagnetic force at this location gradually decreases. At t = 1.2 s, a metal bulge forms and generates a clockwise vortex under surface tension and buoyancy, as shown in [FIGURE:5c]. As time further progresses, the fluid velocity at this location decreases, the weld pool begins to solidify, and the weld reinforcement is formed ([FIGURE:5d]).

[FIGURE:6] and [FIGURE:7] show the calculated temperature and flow fields in the hybrid welding weld pool at a laser power of 500 W. Due to the relatively low laser power density, the effect of vapor recoil force is not significant, and no keyhole forms in the hybrid welding weld pool. Similar to single GMAW welding, a large deformation occurs only in the arc-affected region at the front of the weld pool during welding, and the basic flow patterns in both longitudinal and cross-sections are similar to those in GMAW. However, compared with single GMAW welding, when the laser power is 500 W, no obvious metal accumulation occurs in the hybrid welding weld pool and the humping defect disappears. This may be because the addition of laser energy increases the total heat input, enlarges the liquid weld pool volume, and extends the cooling time, thereby providing sufficient time for the backflow of liquid metal at the rear of the weld pool. Meanwhile, the increased heat flux density raises the temperature of liquid metal in the weld pool, reduces dynamic viscosity, enhances fluidity, and improves weld formation. Additionally, preheating of the workpiece by the leading laser improves the wettability of liquid metal on the workpiece surface, facilitates its lateral spreading, and also suppresses humping defects. It can be seen that even at low power, the presence of laser can effectively suppress humping defects but has little influence on the basic fluid flow pattern in the weld pool, only changing the heat flux distribution characteristics.

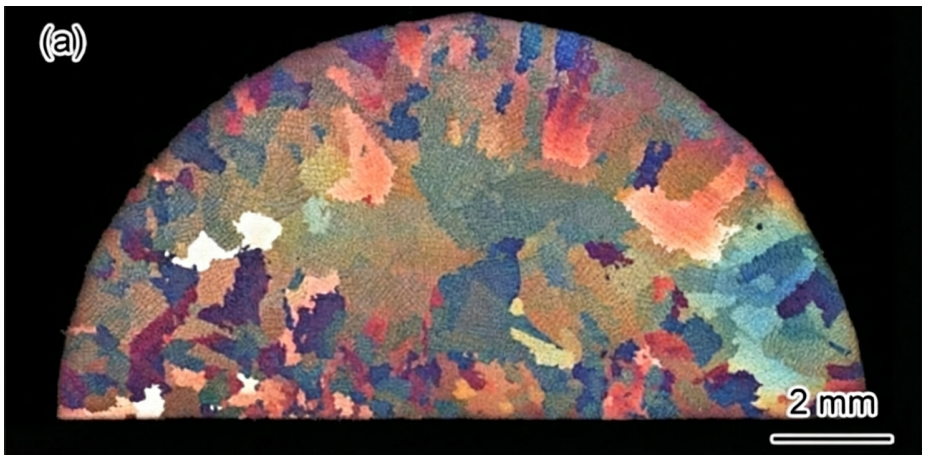

Figure 1: Figure 8

shows the temperature and flow fields in the longitudinal section of the hybrid welding weld pool at a laser power of 2000 W. It can be seen that due to the higher laser power, the effect of laser-induced vapor recoil force increases, and a keyhole appears in the weld pool during welding. The addition of laser energy not only eliminates weld humping defects but also significantly increases the hybrid welding penetration, indicating that at higher laser power, laser heat input has a critical influence on hybrid welding penetration.

Under this condition, the keyhole depth at t = 0.3 s and t = 1.0 s is greater than at t = 0.6 s, meaning the keyhole oscillates during hybrid welding and does not exist stably. This is because the liquid weld pool volume in hybrid welding is large, droplet transfer occurs, and arc pressure, droplet impact force, and electromagnetic force also significantly affect fluid flow in the weld pool. Therefore, the forces on the keyhole wall, especially the rear wall, are difficult to balance, leading to unstable keyhole existence and oscillating keyhole depth. However,

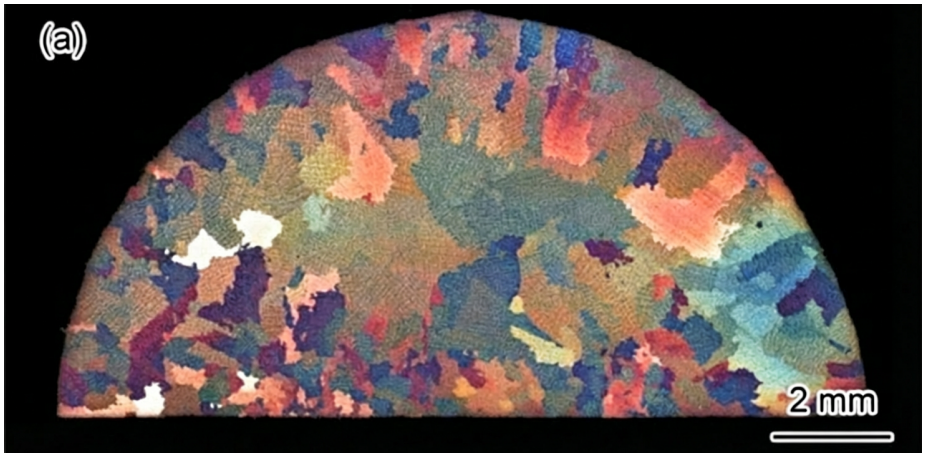

Figure 2: Figure 8

shows that the oscillation range of its depth is basically stable. Additionally, due to the high welding speed in hybrid welding, the keyhole is not symmetric about the laser central axis but tilts obviously backward ([FIGURE:8a] and [FIGURE:8b]), demonstrating the main characteristic of a bent keyhole morphology in high-speed welding [28]. For a bent keyhole, using an axisymmetric laser volume heat source helps to stably apply most of the energy to the front keyhole wall, making its force stability relatively large, which matches the actual physical process in high-speed laser deep penetration welding [28,29]. It can be seen that the model can reflect the main characteristics of keyhole dynamic morphology and its influence on hybrid welding fluid flow.

Further analysis shows that during hybrid welding, a certain depression deformation occurs near the keyhole opening on the weld pool surface under arc pressure,

while fluid velocity near the keyhole wall is relatively large due to vapor recoil force. For the front keyhole wall, since it is subjected to relatively stable vapor recoil force, the velocity of nearby liquid metal is significantly higher than at other locations, reaching a maximum of over 5 m/s, and the liquid metal at this location always flows downward from the keyhole opening to the keyhole bottom, then toward the rear of the weld pool, and upward under buoyancy force. Part of the upward-floating metal flows toward the tail of the weld pool, while part flows back to the front, forming a clockwise vortex in the middle of the weld pool. For the rear keyhole wall, besides vapor recoil force, it is also significantly affected by droplet impact force, arc pressure, and fluid dynamic and static pressures, making its morphology less stable and the flow pattern of nearby liquid metal more complex and related to keyhole dynamic behavior. When the keyhole is deep, the vapor recoil force on the lower part of the rear keyhole wall overcomes surface tension, causing downward flow that merges with the metal flowing backward at the bottom of the weld pool; while the upper metal is more affected by arc pressure, producing upward flow that then moves toward the rear of the weld pool through the pool surface. However, this part of the metal, at a location slightly away from the keyhole, is affected by weld pool impact force, electromagnetic force, and backflowing metal from the rear of the weld pool, and flows downward again toward the bottom of the weld pool before flowing toward the rear, as shown in [FIGURE:8a] and [FIGURE:8c]. When the keyhole is shallow, only upward flow along the rear keyhole wall exists in the nearby liquid metal, as shown in [FIGURE:8b], which is related to the expulsion of downward-flowing front keyhole wall metal and arc pressure.

It can be seen that when the laser power is 2000 W, the presence of the keyhole makes the fluid flow pattern in the longitudinal section of the hybrid welding weld pool very different from that in single GMAW and low-power laser hybrid welding. Under this condition, a relatively stable clockwise flow exists in the weld pool, which helps to bring more arc heat to the bottom of the weld pool, increasing penetration, and also contributes to the uniform distribution of alloying elements from filler metal in the weld pool.

Similarly, the stirring effect of the keyhole changes the cross-sectional morphology and fluid flow pattern of the hybrid welding weld pool. [FIGURE:9] shows the calculated cross-sectional flow field of the hybrid welding weld pool at a laser power of 2000 W. It can be seen that at $t = 0.44$ s, under the influence of arc current, the workpiece metal begins to melt and produces certain surface deformation under arc pressure; while at $t = 0.5$ s, a deeper keyhole forms under vapor recoil force, and fluid in the weld pool flows from top to bottom, with the cross-sectional shape showing characteristics of laser deep penetration welding. As the welding heat source moves, the keyhole at this location is filled with liquid metal and disappears, and the upper width of the weld pool increases due to current heat flux. At $t = 0.8$ s, reinforcement is formed and fluid velocity in the weld pool decreases significantly. The upper part of the weld pool is wide while the lower part is narrow, meaning the cross-section shows characteristics of both GMAW and laser deep penetration welding. At this time, under the influence

of electromagnetic force and weld pool impact force, fluid at the symmetry axis flows from top to bottom. At t = 1.2 s, this location is less affected by arc pressure and electromagnetic force, and under buoyancy, fluid at the symmetry axis flows from bottom to top, forming a clockwise vortex in the upper part of the weld pool under surface tension.

It should be noted that the suppressing effect of laser on humping defects is influenced by welding speed. [FIGURE:10] shows the calculated longitudinal section results of the hybrid welding weld pool at a laser power of 500 W and welding speed of 2 m/min. It can be seen that due to the significantly increased welding speed, the hybrid welding penetration decreases noticeably; meanwhile, the thermal effect of laser on the weld pool relatively weakens, and a certain degree of humping defect reappears in the weld.

[FIGURE:11] and

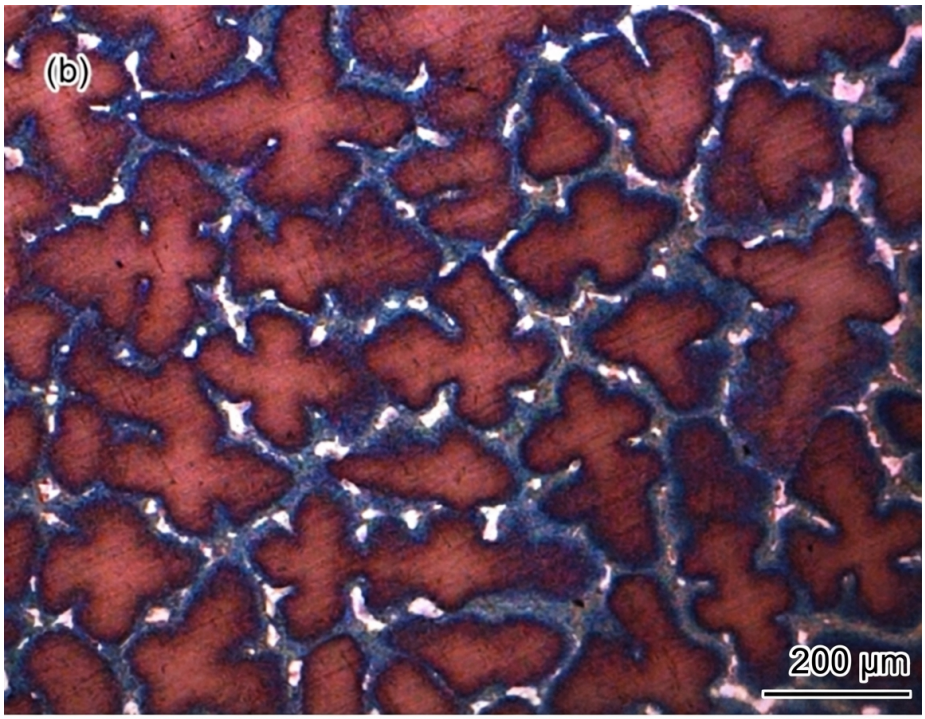

Figure (b): Microstructure of alloy showing dendritic grains (red) and intergranular phase (blue).

Figure 3: Figure 12

compare the experimental and calculated results of the top surface and cross-section of hybrid welding welds at laser powers of 500 and 2000 W. The weld reinforcement is obtained based on the bulge of filler metal, and the specific calculation method for cross-section reinforcement and weld shape dimensions is given in reference [16]. It can be seen that the two agree well, with only some

error in fusion line trend, thereby proving the accuracy and applicability of the established model.

Conclusions

(1) Considering the coupling effects among droplets, weld pool, and keyhole in laser+GMAW hybrid welding, an applicable three-dimensional transient numerical analysis model for keyhole, weld pool fluid flow, and temperature field was established based on FLUENT software.

(2) The fluid flow and temperature field in stainless steel laser+GMAW hybrid welding under different welding conditions were simulated. The calculated weld cross-sectional shapes and dimensions agree well with experimental results, and the model can reflect the main characteristics of hybrid welding fluid flow.

(3) For single GMAW welding (i.e., laser power 0 W) at a welding speed of 1 m/min, metal accumulation occurs in the weld pool, resulting in humping defects in the weld.

(4) For laser+GMAW hybrid welding, when laser power is 500 W at 1 m/min welding speed, no keyhole forms in the weld pool and the basic fluid flow pattern is similar to single GMAW, but weld humping defects disappear; when welding speed increases to 2 m/min, humping reappears.

(5) When laser power is 2000 W at 1 m/min welding speed, a keyhole appears in the hybrid welding weld pool, but its depth is unstable and always oscillating. The metal flow velocity near the front keyhole wall is high and always flows from the keyhole opening to the keyhole bottom. The flow pattern of metal near the rear keyhole wall is related to keyhole dynamic behavior. The keyhole has a strong stirring effect on fluid in the weld pool, with a clockwise vortex always existing in the middle of the weld pool, which helps to bring more arc heat to the bottom of the weld pool and promotes uniform distribution of filler metal alloying elements in the weld pool.

References

[1] Defalco J. Weld J, 2007; 86(10): 47 [2] Graf T, Staufer H. Weld J, 2003; 82(1): 42 [3] Staufer H. Weld J, 2007; 86(10): 36 [4] Bagger C, Olsen F O. J Laser Appl, 2005; 17: 2 [5] Mahrle A, Beyer E. J Laser Appl, 2006; 18: 169 [6] Gao M, Zeng X Y, Hu Q W, Yan J. Trans China Weld Inst, 2008; 29(6): (Gao Ming, Zeng Xiaoyan, Hu Qianwu, Yan Jun. Hanjie Xuebao, 2008; 29(6): 85) [7] Wu C S. Thermal Process and Weld Pool Behavior. Beijing: China Machine Press, 2007: 5 (Wu Chuansong. Hanjie Re Guocheng yu Rongchi Xingtai. Beijing: China Machine Press, 2007: 5) [8] Cho M H, Farson D F. Weld J, 2007; 86(9): 253 [9] Le Guen E, Fabbro R, Carin M, Coste F, Le Masson P. Opt Laser Technol, 2011; 43: 1155 [10] Bendaoud I, Matteï S, Cicala E, Tomashchuk I, Andrzejewski H.

Opt Laser Technol, 2014; 56: 334 [11] Atabaki M M, Nikodinovski P, Chenier P, Liu W, Kovacevic R. Opt Laser Technol, 2014; 59: 68 [12] Xu G X, Wu C S, Qin G L, Wang X Y. Acta Metall Sin, 2012; 48: 1033 (Xu Guoxiang, Wu Chuansong, Qin Guoliang, Wang Xuyou. Jinshu Xuebao, 2012; 48: 1033) [13] Xu G X, Wu C S, Qin G L, Ou H L. China Weld, 2011; 20(1): 22 [14] Xu G X, Wu C S, Qin G L, Wang X Y, Lin S Y. J Eng Manuf, 2011; 225: 528 [15] Xu G X, Wu C S, Qin G L, Wang X Y, Lin S Y. Int J Adv Manuf Technol, 2011; 57: 245 [16] Xu G X, Wu C S, Qin G L, Wang X Y, Lin S Y. Acta Metall Sin, 2009; 45: 107 (Xu Guoxiang, Wu Chuansong, Qin Guoliang, Wang Xuyou, Lin Shangyang. Jinshu Xuebao, 2009; 45: 107) [17] Zhang Z Z, Xu G X, Wu C S. Acta Metall Sin, 2011; 47: 1045 (Zhang Zhuanzhuan, Xu Guoxiang, Wu Chuansong. Jinshu Xuebao, 2011; 47: 1045) [18] Kong F R, Ma J J, Kovacevic R. J Mater Process Technol, 2011; 211: 1102 [19] Xu G X, Wu C S, Qin G L, Wang X Y. Acta Metall Sin (Engl Lett), 2013; 26: 352 [20] Zhang T, Wu C S, Qin G L, Wang X Y, Lin S Y. Comput Mater Sci, 2010; 47: 848 [21] Cho J H, Na S J. Weld J, 2009; 88(2): 35 [22] Cho I W, Na S J, Cho M H, Lee J S. Comput Master Sci, 2010; 49: 172 [23] Zhou J, Tsai H L. Int J Heat Mass Trans, 2008; 51: 4353 [24] Wang R P. PhD Dissertation, Beijing University of Technology, 2011 (Wang Renping. Beijing Gongye Daxue Boshi Xuewei Lunwen, 2011) [25] Gao Z G. PhD Dissertation, Shanghai Jiaotong University, 2009 (Gao Zhiguo. Shanghai Jiaotong Daxue Boshi Xuewei Lunwen, 2009) [26] Zhang T, Wu C S, Feng Y H. Numerical Heat Transfer, 2011; 60A: 685 [27] Voller V R, Prakash C. Int J Heat Mass Transfer, 1987; 30: 1709 [28] Jin X Z, Peter B, Thomas G. J Phys, 2006; 39D: 4703 [29] Semak V V, Matsunawa A. J Phys, 1997; 809D: 30

(Edited by Luo Yanfen)